

# Radiation from low-momentum zoom-whirl orbits

**R. Gold and B. Brügmann**

Friedrich-Schiller University, 07743 Jena, Germany

E-mail: [roman.gold@uni-jena.de](mailto:roman.gold@uni-jena.de), [bernd.bruegmann@uni-jena.de](mailto:bernd.bruegmann@uni-jena.de)

**Abstract.** We study zoom-whirl behaviour of equal mass, non-spinning black hole binaries in full general relativity. The magnitude of the linear momentum of the initial data is fixed to that of a quasi-circular orbit, and its direction is varied. We find a global maximum in radiated energy for a configuration which completes roughly one orbit. The radiated energy in this case exceeds the value of a quasi-circular binary with the same momentum by 15%. The direction parameter only requires minor tuning for the localization of the maximum. There is non-trivial dependence of the energy radiated on eccentricity (several local maxima and minima). Correlations with orbital dynamics shortly before merger are discussed. While being strongly gauge dependent, these findings are intuitive from a physical point of view and support basic ideas about the efficiency of gravitational radiation from a binary system.

PACS numbers: 04.25.Dm, 04.30.Db, 95.30.Sf

## 1. Introduction

Compact binaries, especially black hole binaries, are expected to be primary sources for gravitational wave astronomy. The orbit of a black hole binary is often assumed to be a quasi-circular inspiral that arises after circularization of the orbit due to the emission of gravitational waves, since this is deemed the most likely astrophysical scenario. However, as a matter of principle we should be prepared to detect and recognize gravitational waves from all corners of the parameter space of binaries. So-called zoom-whirl orbits are of particular interest because of their distinct gravitational wave signature, and because in general eccentric orbits can be even more efficient than the quasi-circular inspirals in converting energy of a binary into gravitational waves. Zoom-whirl orbits of a binary are orbits that consist of tight and fast revolutions (the whirls) as well as a phase where the two objects move out to larger distances and back in (the zooms).

The basic features of zoom-whirl orbits were first discussed in the context of geodesics in a stationary black hole spacetime. This describes the limit of a small test mass moving around a large central black hole, see for example [1–7], some of which include radiation effects. The main question in full general relativity is how the classic, well-known picture of zoom-whirl geodesics changes for binaries with comparable masses in configurations where radiation damping becomes significant. *A priori* it is unclear how many whirls can be achieved by fine-tuning the initial orbital parameters (arbitrarily many in the case of geodesics) since the system is quickly losing energy and angular momentum. If little tuning is involved, then zoom-whirl orbits can be potential GW sources even for ground-based detectors, see for example [8–11].

Recently, zoom-whirl orbits have become the subject of numerical simulations in full general relativity. In [12], Pretorius and Khurana presented the first example of a whirl orbit of an equal mass black hole binary. In [13–15], several examples for the transition from inspiral to plunge, radiated energy and angular momentum have been studied. In [8], up to three whirl phases have been found. The first study of binaries with non-vanishing spin can be found in [16], and the consequences for kicks have been studied in [17]. The focus in [18–20] is on high-energy collisions, where the kinetic energy becomes the dominant contribution to the total mass of the system.

In this paper we examine one particular type of zoom-whirl orbit for equal masses and vanishing spin. The magnitude of the linear momentum of the initial data is fixed to that of a quasi-circular orbit at the given initial separation, and its direction is varied. With our choice of initial data we probe a comparatively low-momentum regime aiming at astrophysically reasonably realistic binaries. Similar low-momentum cases have been studied in [8]. The novel aspect of the present work is that we perform a detailed investigation of how the energy radiated depends on the initial angle and find a physical interpretation of this dependence. Main result is that there is not just one maximum in the radiated energy as a function of the initial angle. Rather, several local maxima and minima can be identified, which should be compared to the variations in the mass and spin of the merger remnant noted in [16]. We link these extrema to the motion of the punctures. Furthermore, for this low-momentum case, the amount of fine-tuning required is small; an angular resolution of about  $1^\circ$  suffices.

The term ‘zoom-whirl’ has obvious meaning when several or more whirl orbits near an (unstable) quasi-circular orbit are found, but recent literature colloquially refers to orbits with one or two whirls also as ‘zoom-whirl’ orbits. The physics behind the whirls is precession, and any eccentric orbit has some amount of precession. This begs the question at what point large precession becomes a whirl. We refer to an orbit as a zoom-whirl orbit if at least one whirl orbit is completed before the next zoom, i.e. if from one apoastron of a zoom to the next an additional angle of  $2\pi$  or more is traversed. However, in order to distinguish large precession on the order of  $\pi$  that occurs for certain black hole mergers (as discussed in this paper) from perturbative precession effects on the order of arcseconds, we refer to precession effects on the order of  $\pi$  also as partial or fractional whirls.

## 2. Numerical Computations

We perform a parameter study of equal mass, nonspinning black hole binaries by varying the direction of the initial momentum (see below). We use the BAM-code [21, 22] to solve the full Einstein equations in vacuum. The problem is cast as a Cauchy-initial-value problem by foliating the four dimensional spacetime into families of three-dimensional hypersurfaces labeled by a coordinate time  $t$ . Initial data for the initial hypersurface are obtained by the puncture method using a pseudo-spectral code [23, 24] assuming the spacetime being conformally flat. The computational method uses adaptive mesh refinement (typically 7 – 10 levels) together with Berger-Oliger timestepping. We use the  $\chi$ -variant of the moving-puncture [25, 26] version of the Baumgarte-Shapiro-Shibata-Nakamura (BSSN) formulation [27, 28]. The runs are performed with sixth-order finite differencing in space [29] and a fourth-order Runge-Kutta method. For the purpose of wave extraction we use an implementation of the Newman-Penrose formalism which is also fourth order accurate. We can demonstrate consistent, overall fourth-order convergence in the 22-mode of  $r\Psi_4$  and the radiated

energy  $E_{rad}$  with typical relative errors of  $1 - 2\%$  for  $E_{rad}$  and slightly less than  $1\%$  for the 22-mode. The error due to a finite extraction radius was estimated by extracting the waves at different radii  $r = 60M, 80M, 100M$  (where  $M$  is the total puncture mass) and computing the deviations from the expected  $1/r$  fall-off. This error turned out to be roughly of the same order as the discretization error mentioned above.

Two punctures of mass  $m$  are placed on the  $x$ -axis at  $x_1 = -10M$  and  $x_2 = +10M$ , respectively, where  $M = 2m$ , so that the initial coordinate separation is  $D = 20M$ . The magnitude  $P$  of the linear momentum  $\vec{P}$  of each puncture is set equal to the value for quasi-circular orbits,  $P = P_{qc} = 0.061747M$ , using the methods of [30]. We systematically vary the direction of  $\vec{P}$ , which implies corresponding changes in the initial angular momentum and also the eccentricity of the orbit. This is parameterized by a shooting angle  $\Theta$  defined as the angle spanned by the initial linear momentum vector  $\vec{P}$  and the  $x$ -axis. Alternatively, we could e.g. vary the size of the initial momentum, which we leave for a future investigation. Varying the values of  $\Theta$  from  $\Theta = 30^\circ$  to  $\Theta = 53^\circ$  we compute  $E_{rad}$  and investigate how the energy might be related to the trajectories of the punctures. This study involves 24 binary black hole evolutions, plus convergence runs.

### 3. Results

We analyze the dependence of the radiated energy  $E_{rad}$  on the shooting angle  $\Theta$  and observe new features for eccentric, equal-mass and non-spinning binary black holes including zoom-whirl behaviour. The results on radiated energy are summarized in figure 1. Figure 2 compares two of the waveforms, and the full orbital trajectories of three representative cases are shown in figure 3.

First, we note that for the size of the linear momentum considered here eccentric black hole binaries can be significantly (15%), but not drastically more efficient than quasi-circular binaries in converting initial energy into outgoing gravitational radiation. This can also be seen from figure 2, where we plot the  $l = 2, m = 2$  mode of  $r\mathcal{Re}(\Psi_4)$  for the  $\Theta = 47^\circ$  run against a quasi-circular waveform. Especially at the onset of merger the amplitude of the eccentric waveform is significantly larger than in the quasi-circular case. This will be further explored in an upcoming work in the context of larger initial momenta. Second, for  $\Theta$  in the range of  $45^\circ - 53^\circ$ ,  $E_{rad}$  fluctuates between  $0.04M_{ADM}$  and  $0.05M_{ADM}$ . The oscillations are much larger than the estimated relative numerical error of  $1 - 2\%$ , and are therefore considered a feature of the physics rather than a numerical artefact. Analogous variations have been observed in the mass of the merger remnant as well as in the final spin in [16]. However, these oscillatory features have not been observed by [14, 18], while the behaviour for low  $\Theta$  looks very similar to [13]. In the following we will explore the origin of the above findings in more detail.

We find strong evidence that the local minima and maxima are linked to different types of dynamics near the merger. In order to make a more precise statement we define the coordinate separation vector  $\vec{S}$  pointing from one puncture to the other with length  $|\vec{S}(t)| = D(t)$  for all  $t$ , and we denote the time when a common horizon is formed by  $t_{merger}$ . We depict the following observation in figure 4. Whenever the tangent vector of the puncture orbit is closest to being orthogonal to  $\vec{S}(t = t_{merger})$  then the corresponding orbit turns out to maximize the radiated energy compared to other evolutions in the neighbourhood in parameter space. In contrast, those orbits

whose tangent vectors point furthest inwards at the onset of merger (e.g.  $\Theta = 48^\circ$ , dotted line in figure 4) minimize the radiated energy. Figure 5 shows the angle at merger time for a number of different runs. The locations of the maxima and minima in figure 5 mimic the dependence of the energy on the shooting angle shown in figure 1.

A physical interpretation of this effect is intrinsically complicated due to the high degree of gauge dependence in this highly nonlinear region in spacetime. Nevertheless, the above-mentioned effect might originate from the fact that initial eccentricities within a certain range can maximize or minimize the time the binary spends in the radiatively most efficient configuration, namely small separations and high velocities. It is rather intuitive that orbits with radial velocity  $v_r \approx 0$  shortly before merger (e.g.  $\Theta = 47^\circ$ , solid line in figure 4) spend comparatively more time in a radiatively-efficient zone than in the case where  $v_r$  is larger. A large  $v_r$  leads to a rapid rush through this crucial zone leaving the binary less time to radiate.

This interpretation is further supported by the data shown in figure 6. In this plot we compute a histogram of  $D = D(t)$ , i.e. we count the number of time steps during which the coordinate separation of the binary lies within each bin of width  $\Delta D$ , thereby visualizing how much time the binary spends at a given separation  $D$ . First, we observe that we can define the radius for innermost unstable circular orbits rather well for our gauge-choice, because in this plot they show up as a sharp and strong peak. Second, the comparison between the upper and lower panel confirm our interpretation, that more efficient runs spend more time in a radiatively-efficient zone than less efficient binaries. In this plot the emission zone corresponds to a band bounded on the left by  $D_{\text{Merger}}$ , which is defined as the coordinate separation at which a common horizon forms. We find  $D_{\text{Merger}} = (1.8 \pm 0.1)M$ . We want to check to what degree the above hypothesis withstands the issue of gauge dependence in an upcoming work. The idea is to further investigate the momentum dependence (which the gauge is sensitive to) and work out other diagnostics in order to clarify whether or not such arguments carry over to more general scenarios.

Concerning the phenomenology of the orbital dynamics and the radiated energy, we should emphasize that the maximum in radiated energy corresponds to an evolution which only completes about 1.3 orbits before merger, i.e. the orbit is highly eccentric. (A 3PN [31] estimate for  $\Theta = 48^\circ$  gives  $e \approx 0.8$ .) For  $48^\circ \leq \Theta \leq 48.5^\circ$ , i.e. near one of the minima and not at one of the maxima, the orbits exhibit a ‘whirl’ phase slightly before merger. This whirl phase does not seem to be the most relevant moment for wave emission since we find that this almost circular motion happens at a much larger radius (which depends inversely on the eccentricity) than the coordinate separation at merger (see figure 6). This argument is supported by the observation that the orbits which manage to whirl, but do not exhibit a zoom *minimize*  $E_{\text{rad}}$ . For  $\Theta = 48.5^\circ$  the whirl phase is followed by a very small ‘zoom’. Above that value for  $\Theta$  the whirl phase becomes shorter and the zooms larger (note the prominent zoom of the  $\Theta = 50^\circ$  run (dashed line) in figure 3), and for  $\Theta > 52^\circ$  there are multiple subsequent close encounters (or fractional whirls) before the final merger.

In the strong field regime, the precise definition of eccentricity and precession is problematic. Furthermore, the precession of the orbit is no longer proportional to the eccentricity. For a large range of shooting angles (eccentricities) the precession becomes a significant fraction of  $2\pi$  and for a small range it even exceeds  $2\pi$ . This is one of the main results of our (and other) investigations. Prior to numerical simulations it was not clear whether zoom-whirl behaviour exists at all in non-spinning, equal mass binaries. Indeed, as we demonstrate, the range where full whirls occur is very

limited, and the more typical phenomenology is rather governed by a strong form of precession. The transition from close encounters to zoom-whirls is completely smooth, and we especially want to highlight that there is no significant fine-tuning involved beyond about  $1^\circ$  in the shooting angle.

The expectation that a high degree of fine-tuning may be required originates with the search for geodesics that complete a large number of whirls. These are typically found near an unstable circular orbit (inside the radius of the innermost stable circular orbit), which suggests that due to the instability a high degree of fine-tuning is required. Also, the more time is spent in the whirl, the stronger the dependence on the initial parameters. In our case, only about one full whirl is found, so the sensitivity on the initial angle should be modest. Furthermore, although the whirl occurs near an unstable orbit with a diameter of  $3.5M$  (figure 3), the degree of instability seems to be sufficiently mild to require only a small amount of fine-tuning.

These findings are very different from the high energy case [12, 18], where furthermore evidence for critical scaling around the so-called threshold of immediate merger has been found. In this regime highly fine-tuned initial conditions are necessary. We plan to investigate larger momenta in future work.

### Acknowledgments

The authors wish to thank M. Campanelli, L. Gergely, J. Grigsby, D. Hilditch, J. Levin, D. Müller, G. Schäfer, D. Shoemaker and U. Sperhake for discussions. This work was supported in part by DFG SFB/Transregio 7 and DFG Research Training Group 1523. The computations were carried out on the HLRB2 system at the LRZ in Garching.

### References

- [1] S. Chandrasekhar. *The Mathematical Theory of Black Holes*. Oxford University Press, USA, 1983.
- [2] Karl Martel. Gravitational waveforms from a point particle orbiting a schwarzschild black hole. *Physical Review D*, 69:044025, 2004.
- [3] Janna Levin and Becky Grossman. Dynamics of black hole pairs i: Periodic tables. *Physical Review D*, 79:043016, 2009.
- [4] Rebecca Grossman and Janna Levin. Dynamics of black hole pairs ii: Spherical orbits and the homoclinic limit of zoom-whirliness. *Physical Review D*, 79:043017, 2009.
- [5] Curt Cutler, Daniel Kennefick, and Eric Poisson. Gravitational radiation reaction for bound motion around a schwarzschild black hole. *Phys. Rev. D*, 50(6):3816–3835, Sep 1994.
- [6] Kostas Glampedakis and Daniel Kennefick. Zoom and whirl: eccentric equatorial orbits around spinning black holes and their evolution under gravitational radiation reaction. *Phys. Rev.*, D66:044002, 2002.
- [7] Scott A. Hughes, Steve Drasco, Eanna E. Flanagan, and Joel Franklin. Gravitational radiation reaction and inspiral waveforms in the adiabatic limit. *Physical Review Letters*, 94:221101, 2005.
- [8] James Healy, Janna Levin, and Deirdre Shoemaker. Zoom-whirl orbits in black hole binaries. *Phys. Rev. Lett.*, 103(13):131101, Sep 2009.
- [9] Karl Martel and Eric Poisson. Gravitational waves from eccentric compact binaries: Reduction in signal-to-noise ratio due to nonoptimal signal processing. *Physical Review D*, 60:124008, 1999.
- [10] Duncan A. Brown and Peter J. Zimmerman. Effect of eccentricity on searches for gravitational waves from coalescing compact binaries in ground-based detectors. *Phys. Rev. D*, 81(2):024007, Jan 2010.
- [11] Linqing Wen. On the Eccentricity Distribution of Coalescing Black Hole Binaries Driven by the Kozai Mechanism in Globular Clusters. *Astrophys. J.*, 598:419–430, 2003.

- [12] Frans Pretorius and Deepak Khurana. Black hole mergers and unstable circular orbits. *Class. Quant. Grav.*, 24:S83–S108, 2007.
- [13] U. Sperhake, E. Berti, V. Cardoso, J. A. Gonzalez, B. Bruegmann, and M. Ansorg. Eccentric binary black-hole mergers: The transition from inspiral to plunge in general relativity. *Physical Review D*, 78:064069, 2008.
- [14] Ian Hinder, Birjoo Vaishnav, Frank Herrmann, Deirdre Shoemaker, and Pablo Laguna. Circularization and final spin in eccentric binary black hole inspirals. *Physical Review D*, 77:081502, 2008.
- [15] M. C. Washik, J. Healy, F. Herrmann, I. Hinder, D. M. Shoemaker, P. Laguna, and R. A. Matzner. Binary black hole encounters, gravitational bursts and maximum final spin. *Physical Review Letters*, 101:061102, 2008.
- [16] James Healy, Pablo Laguna, Richard A. Matzner, and Deirdre M. Shoemaker. Final mass and maximum spin of merged black holes and the golden black hole. *Phys. Rev. D*, 81(8):081501, Apr 2010.
- [17] James Healy, Frank Herrmann, Ian Hinder, Deirdre M. Shoemaker, Pablo Laguna, and Richard A. Matzner. Superkicks in hyperbolic encounters of binary black holes. *Physical Review Letters*, 102:041101, 2009.
- [18] Ulrich Sperhake, Vitor Cardoso, Frans Pretorius, Emanuele Berti, Tanja Hinderer, and Nicolas Yunes. Cross section, final spin, and zoom-whirl behavior in high-energy black-hole collisions. *Phys. Rev. Lett.*, 103(13):131102, Sep 2009.
- [19] U. Sperhake, V. Cardoso, F. Pretorius, E. Berti, and J. A. Gonzalez. The high-energy collision of two black holes. *Physical Review Letters*, 101:161101, 2008.
- [20] Masaru Shibata, Hirotada Okawa, and Tetsuro Yamamoto. High-velocity collision of two black holes. *Phys. Rev.*, D78:101501, 2008.
- [21] Bernd Brügmann, Wolfgang Tichy, and Nina Jansen. Numerical simulation of orbiting black holes. *Phys. Rev. Lett.*, 92:211101, 2004.
- [22] Bernd Brügmann, José A. González, Mark Hannam, Sascha Husa, Ulrich Sperhake, and Wolfgang Tichy. Calibration of moving puncture simulations. *Phys. Rev. D*, 77:024027, 2008.
- [23] S. Brandt and B. Brügmann. A simple construction of initial data for multiple black holes. *Phys. Rev. Lett.*, 78(19):3606–3609, 1997.
- [24] Marcus Ansorg, Bernd Brügmann, and Wolfgang Tichy. A single-domain spectral method for black hole puncture data. *Phys. Rev. D*, 70:064011, 2004.
- [25] Manuela Campanelli, Carlos O. Lousto, Pedro Marronetti, and Yosef Zlochower. Accurate evolutions of orbiting black-hole binaries without excision. *Phys. Rev. Lett.*, 96:111101, 2006.
- [26] John G. Baker, Joan Centrella, Dae-Il Choi, Michael Koppitz, and James van Meter. Gravitational wave extraction from an inspiraling configuration of merging black holes. *Phys. Rev. Lett.*, 96:111102, 2006.
- [27] M. Shibata and T. Nakamura. Evolution of three-dimensional gravitational waves: Harmonic slicing case. *Phys. Rev. D*, 52:5428–5444, 1995.
- [28] T. W. Baumgarte and S. L. Shapiro. On the Numerical integration of Einstein’s field equations. *Phys. Rev. D*, 59:024007, 1998.
- [29] Sascha Husa, José A. González, Mark Hannam, Bernd Brügmann, and Ulrich Sperhake. Reducing phase error in long numerical binary black hole evolutions with sixth order finite differencing. *Class. Quantum Grav.*, 25:105006, 2008.
- [30] Benny Walther, Bernd Brügmann, and Doreen Müller. Numerical black hole initial data with low eccentricity based on post-Newtonian orbital parameters. *Phys. Rev.*, D79:124040, 2009.
- [31] Raoul-Martin Memmesheimer and Gerhard Schaefer. Third post-newtonian constrained canonical dynamics for binary point masses in harmonic coordinates. *Physical Review D*, 71:044021, 2005.

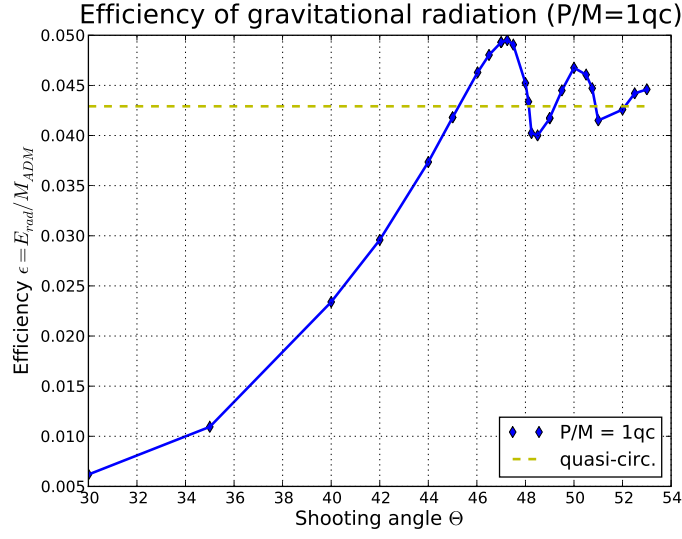


**Figure 1.** Efficiency of gravitational radiation as a function of the shooting angle  $\Theta$ . For the  $y$ -axis we normalize  $E_{rad}$  by the ADM-mass of the initial time slice. The maximum at  $\Theta \approx 47^\circ$  corresponds to an initial orbital angular momentum  $L = DP \sin(\Theta) = 0.88M^2$ .

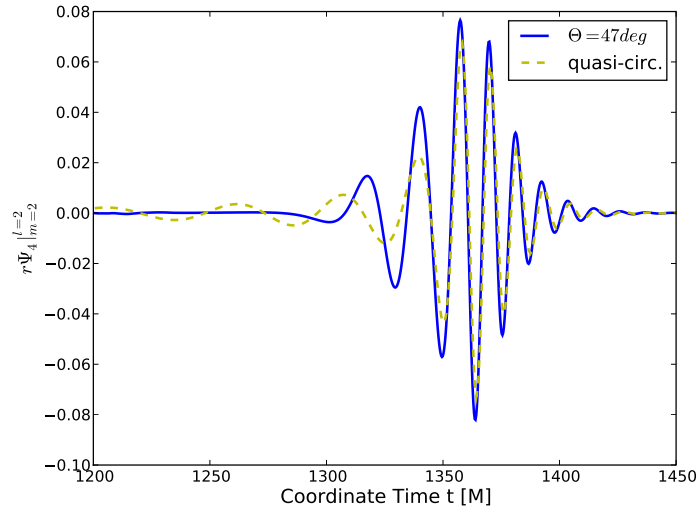


**Figure 2.** Comparison of 22-modes of the most efficient case ( $\Theta = 47^\circ$ ) and the quasi-circular ( $\Theta = 90^\circ$ ) case. The late-time, ring-down waveforms are quite similar. Differences are visible before the merger where the amplitude for the  $\Theta = 47^\circ$  case is up to twice as large as for the quasi-circular binary, and in the inspiral part where the quasi-circular orbit results in more radiation.

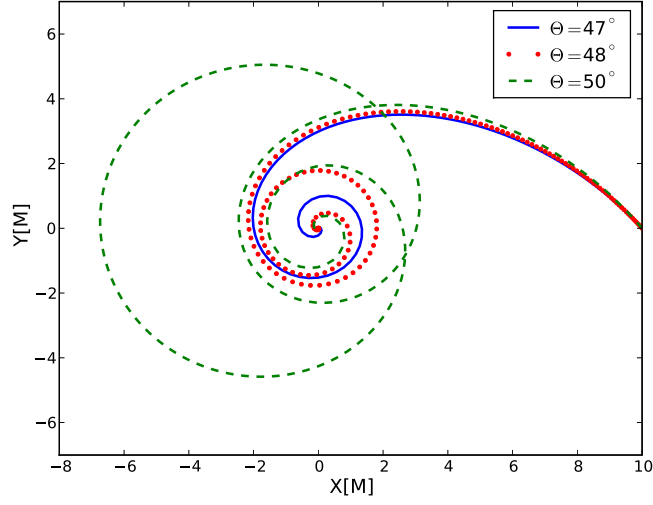


**Figure 3.** Trajectories of three evolutions corresponding to one minimum and two maxima in  $E_{rad}$  (compare  $\Theta$  values in the legend with  $x$ -axis in figure 1). The solid line represents an inspiral without noticeable whirl or zoom, the dotted line shows a complete whirl before the plunge, and the dashed line starts with a fractional whirl (less than a full whirl orbit but strong precession), followed by a zoom phase and the plunge. Only one puncture trajectory for each evolution is shown for clarity.

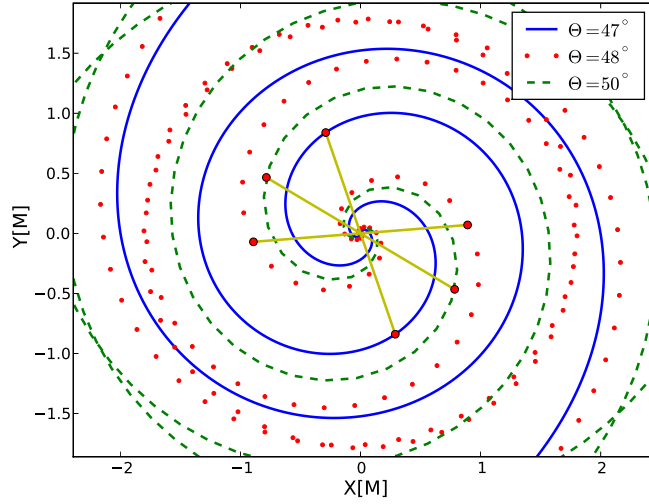


**Figure 4.** Zoom into the inner part of three orbital evolutions corresponding to one minimum and two maxima in  $E_{rad}$  (compare  $\Theta$  values in the legend with  $x$ -axis in figure 1). The markers denote the onset of merger. A maximum in  $E_{rad}$  occurs when the coordinate separation vector  $\vec{S}$  (straight line) is closest to being orthogonal to the tangent vector of the puncture tracks at the time of merger.



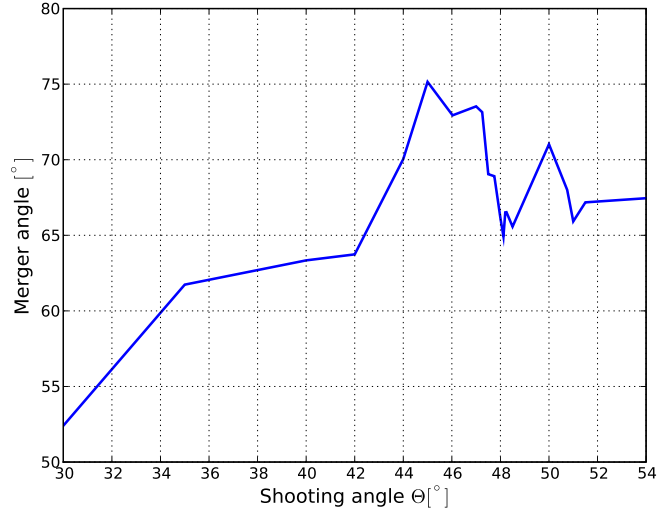


**Figure 5.** The angle between the tangent vector of the puncture orbit and the separation vector  $D$  as a function of the initial shooting angle. This plot looks similar in its general shape to the plot for the radiated energy in figure 1. The locations of the maxima and minima basically coincide.

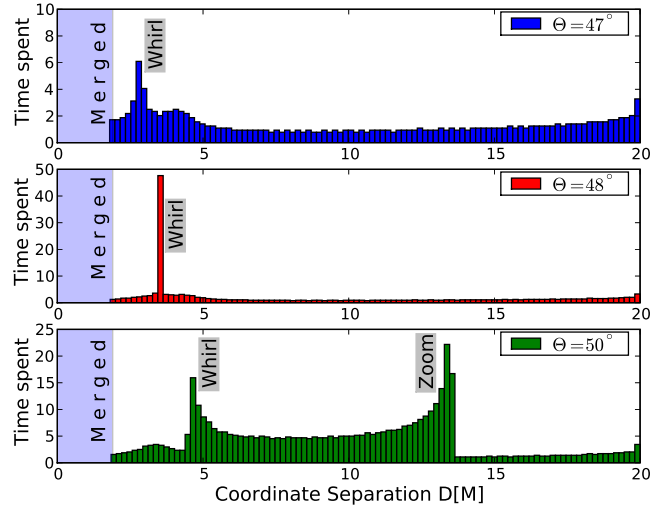


**Figure 6.** Another comparison regarding efficiency using a histogram of  $D$ . Shown is how much time the binary has spent at  $D \pm 0.2$ . The histograms include data up until the merger time  $t_{\text{merger}}$  which read  $137M$ ,  $184M$  and  $432M$ , upper to lower, respectively. Less efficient binaries (middle panel) spent more time at a larger separation whereas efficient ones (upper panel) at lower separations. In the lower panel one can see that both whirl and zooms cause peaks in this diagram.